

Reindeer carcasses modulate vegetation composition and greenness in High-Arctic tundra

Maya Nisha Situnayake ^a, Marit By ^a, Oddbjørn Larsen ^a, Stijn Sombekke ^b, Lammert Kooistra ^b, Raket Blaallid ^a, Jan Eivind Østnes ^a, Nuria Selva ^{c,d,e}, Åshild Ønvik Pedersen ^f, and Sam M.J.G. Steyaert ^a

^aTerrestrial Ecology Group, Faculty of Biosciences and Aquaculture, Nord University, NO-7715 Steinkjer, Norway; ^bLaboratory of Geo-Information Science and Remote Sensing, Wageningen University and Research, 6700AA Wageningen, The Netherlands; ^cInstitute of Nature Conservation, Polish Academy of Sciences, 31-120 Krakow, Poland; ^dDepartamento de Ciencias Integradas, Facultad de Ciencias Experimentales, Centro de Estudios Avanzados en Física, Matemáticas y Computación, Universidad de Huelva, 21071 Huelva, Spain; ^eEstación Biológica de Doñana, Consejo Superior de Investigaciones Científicas, 41092 Sevilla, Spain; ^fNorwegian Polar Institute, Fram Centre, Post box 6606 Stakkevollan, NO-9296, Tromsø, Norway

Corresponding author: Maya Nisha Situnayake (email: maya.n.situnayake@nord.no)

Abstract

Vertebrate carrion is an integral part of foodwebs in ecosystems and can impact biodiversity at the local as well as the landscape scale. However, very little knowledge currently exists about the ecological role of carrion in the Arctic ecosystems. We conducted a ground survey on the cover of five plant functional groups at paired reindeer carcass and control sites and analysed the relationship between cover and carcass presence in the Arctic tundra of Svalbard. Vegetation indices from Red-Green-Blue (RGB) imagery captured by drones complemented this, assessing plant productivity in terms of “spectral greening” and modelling the relationship between vegetation index values and carcass distance. We show that graminoids capitalised most from carcass presence, whereas bryophytes and lichen showed decreases in cover. Woody plant and forb covers were not significantly impacted by carcass presence. The Red Green Blue Vegetation Index decreased locally at fresh carcasses (i.e., <1 year old) but showed an increase at more established carcass sites (i.e., >1 year). We show that carcasses have differential impacts on the plant functional groups of Svalbard’s tundra and induce a local “green-up” through secondary succession within 2 m of the carcass. Given their non-random distribution, carcasses may contribute to vegetation heterogeneity at landscape scales. This is relevant for understanding how climate change-induced reindeer mortalities will impact tundra plant community composition in the future.

Key words: carcass ecology, drone, remote sensing, tundra, vegetation index

Introduction

Dead organic matter from animals, or carrion, is a high-quality resource that can structure and stabilise food-webs in both terrestrial and aquatic ecosystems (Wilson and Wolkovich 2011; Beasley et al. 2012; Barton et al. 2013; Benbow et al. 2019). Vertebrate carrion is nutritionally rich, with carbon:nitrogen ratios often magnitudes lower compared to most dung and plant debris (Carter et al. 2007; Barton et al. 2013; Benbow et al. 2019). Consequently, it is an attractive resource for many, and typically aggregates organisms from various life-forms, functioning as biodiversity hotspots that facilitate ecological interactions between species and kingdoms (Barton et al. 2013; Olea et al. 2019a). The ecological relevance of carrion in ecosystem functioning has long been overlooked but is now becoming widely acknowledged (Moleón and Sánchez-Zapata 2015; Benbow et al. 2015b); however, important knowledge gaps still exist such as the ecosystem context of carcass-induced ecological effects (Barton et al. 2013), and how much carrion is available in

ecosystems (Bump et al. 2020), especially in the Arctic (Olea et al. 2019b).

With death, animal tissue that developed during an individual’s time alive and across a relatively large space (e.g., home range, territory) suddenly becomes available for decomposition and consumption at a discrete point in space, at least in terrestrial ecosystems (Carter et al. 2007; Beasley et al. 2012). Since processes that provide carrion (e.g., predation, hunting, traffic collisions) are typically not randomly distributed in space (Bump et al. 2009a; Steyaert et al. 2016; Hegland and Hamre 2018), carrion can occur spatially structured and hence maintain or enhance diversity and heterogeneity at landscape or ecosystem scales (Towne 2000; Bump et al. 2009a). Carcasses of larger vertebrates typically induce a biogeochemical disturbance in both above- and below-ground communities and soil chemistry. The influx of nutrients from microorganismal decomposition, combined with necrophagous insect and vertebrate scavenger activity, generally leave a carcass decomposition site that becomes locally

denuded of vegetation. Such sites with nutrient-enriched soils and altered vegetation cover are often referred to as “cadaver decomposition islands” (CDIs) (Carter et al. 2007). CDIs offer opportunities for various plant life that would otherwise not establish (Bump et al. 2009b; Steyaert et al. 2018; Arnberg et al. 2022, 2024), and which green-up during secondary succession (i.e., the re-establishment of vegetation over time after disturbance, for example induced by the presence of a carcass). Eventually, CDIs can turn into lush patches that can be distinguished from their surroundings for prolonged periods of time (Towne 2000; Carter et al. 2007; Bump et al. 2009b). Carrion decomposition is, however, highly dependent on the environmental context. For example, temperature modulates competition between microorganismal decomposers, necrophagous arthropods, and vertebrate scavengers for carrion resources (DeVault et al. 2004). By reducing competition with decomposers and invertebrates, colder temperatures appear to favour vertebrate scavengers (DeVault et al. 2004), which disperse carrion biomass across the landscape, thereby diluting local impacts of carrion on soil and vegetation (DeVault et al. 2004; Beasley et al. 2015). Much carrion biomass remains in situ through decomposition by microorganisms and arthropods (Benbow et al. 2015a), which in turn can have larger local effects on third parties, such as vegetation and communities, which do not directly consume carrion (Moleon et al. 2014). Other factors that can affect carrion fate include moisture regime, vegetation type, vertebrate community structure, and carrion management (e.g., removal and destruction) (Janzen 1977; DeVault et al. 2004; Selva et al. 2005).

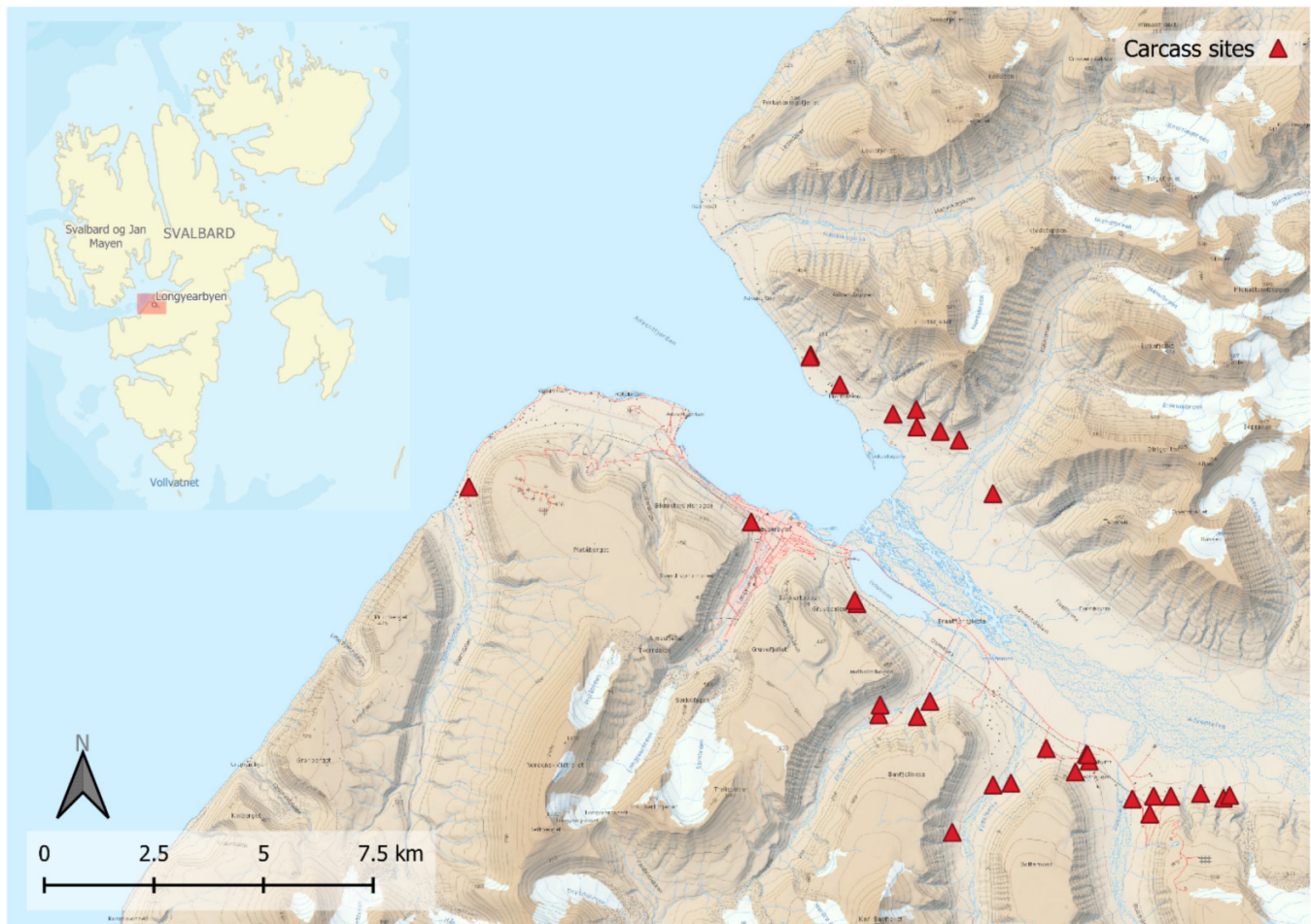
Arctic tundra is characterised by short growing seasons and limited active layer depth. Nutrient limitation and moisture are also important restricting factors for primary production (Billings 1987; Mack et al. 2004; Myers-Smith et al. 2011; Mekonnen et al. 2021). Hence, nutrient inputs from carrion can have profound and long-lasting impacts on vegetation, albeit on a local scale. Indeed, Danell et al. (2002) showed that muskox (*Ovibos moschatus*) carcasses (>5 years old) in the Arctic tundra facilitated vigorous plant growth, and that plant material had elevated nitrogen concentrations up to about 2 m from the carcasses for prolonged periods of time, highlighting that despite a limited sample size ($N = 4$), how vertebrate carrion can play an important role in vegetation dynamics in the Arctic tundra. Increased nutrient supply generally stimulates plant production, but nutrient excess, for example, due to carrion decomposition, can cease growth, damage plant tissue, and be lethal (Goyal and Huffaker 1984; Carter et al. 2007). Responses to nutrient excess can vary tremendously between functional groups. For example, several studies have shown that graminoids (members within the families Poaceae, Cyperaceae, and Juncaceae) and other herbaceous plants (other flowering plants without true woody tissue), here called forbs, increase in overall productivity during secondary succession induced by carrion decomposition (Towne 2000; Danell et al. 2002; van Klink et al. 2020). However, for forbs, responses appear to be more ambiguous and vary across ecosystems and life strategies (Towne 2000; Bump et al. 2009b). Towne

(2000) reported that woody vegetation and annual grasses were not substantially affected by carcasses. However, several studies show that the carrion-induced disturbances generate recruitment windows of opportunity for various woody plants (Bump et al. 2009b), including alpine tundra ecosystems (Steyaert et al. 2018; Arnberg et al. 2022). Arnberg et al. (2022) furthermore reported that bryophyte and lichen cover decreased as a response to carrion in an alpine tundra ecosystem.

Vegetation studies typically rely on field surveys to collect data on, for example, plant community structure, biomass, or nutrient content (Chytrý et al. 2011; Eischeid et al. 2021). The vast and remote landscapes of the Arctic make traditional field data collection challenging; however, unmanned aerial vehicles or drones are becoming affordable and important complementary research tools in ecology, particularly for vegetation studies (Cruzan et al. 2016; Eischeid et al. 2021). Drones can be equipped with a variety of sensors (e.g., multispectral cameras, thermal sensors, etc.) and are flexible in terms of timing of deployment and flight altitudes, although their use is restricted by weather conditions (e.g., precipitation, strong winds), battery life, and legislation (Duffy et al. 2017). Many off-the-shelf-drones currently come with a photo/video camera that records imagery in the visible part of the electromagnetic spectrum (i.e., Red–Green–Blue (RGB) or the red, green, and blue bands in imagery). Such drones can complement field survey data with high-resolution imagery, which can be used, for example, to produce vegetation classification maps (Hamylton et al. 2020; Eischeid et al. 2021), object detection (Xia et al. 2022), or to produce spectral vegetation indices (Zhang et al. 2019). Spectral vegetation indices combine values of two or more spectral bands of imagery into one single band or raster, of which the pixel values correlate with specific vegetation properties (Myneni et al. 1995; Chuvieco 2016). Many (multi)spectral vegetation indices have been designed over the last decades, where the Normalised Difference Vegetation Index (NDVI) is the most common one as it correlates well with chlorophyll content in vegetation (i.e., vegetation “greenness”) (Pettoirelli et al. 2005).

In this study, we evaluate responses of plant functional groups and “greenness” to large vertebrate carrion in the Arctic tundra. Within our study system in Svalbard, only one large herbivore species is present, the Svalbard reindeer (*Rangifer tarandus platyrhynchus*). Mortality takes place mostly among young and old individuals during late winter or early spring due to starvation (Reimers 1983; Hansen et al. 2011). Extreme weather events such as warm spells with rain-on-snow events create impenetrable ice sheets that limit reindeer access to food resources and have been directly associated with reindeer mortality on Svalbard (Hansen et al. 2011, 2014; Peeters et al. 2019). We took advantage of a long-term reindeer monitoring dataset that includes reindeer carcass information to investigate vegetation responses of high Arctic tundra vegetation to large vertebrate carrion. We hypothesise that carcasses will have differential impacts on plant functional groups. We expect that graminoids will overall increase as a response to reindeer carcasses (Danell et al. 2002), whereas bryophyte and lichen cover will decrease (Arnberg

Fig. 1. Overview of the study area with each reindeer carcass site ($N = 33$) indicated by a red triangle (basemap: Norwegian Polar Institute n.d.). The smaller map insert (upper left) shows the location of the study area in the wider context of the Svalbard archipelago (basemap: Esri, World Street Map; Esri 2024). Both the map projection and coordinate system of data plotted is WGS 84/UTM 33N (ESPG: 32633).



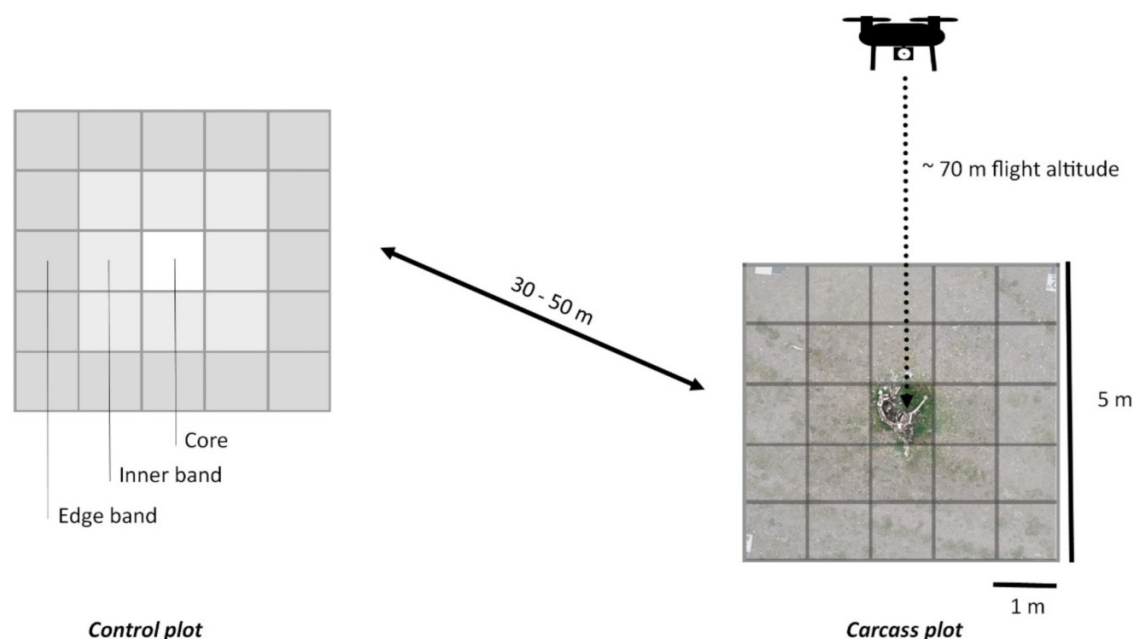
et al. 2022). We do not expect a clear impact of reindeer carcasses on woody vegetation cover (Towne 2000). Responses of forb species to carrion decomposition are not straightforward according to the literature (Towne 2000; Dormann and Woodin 2002; Bump et al. 2009b). However, our field observations from both Alpine and Arctic tundra suggest that forb cover increases at carcass sites, especially during later successional stages. As shown in several other studies (e.g., Towne 2000; Danell et al. 2002), we expect that the anticipated effects will be very local, not extending more than a few metres from the carcass (i.e., 1–3 m). We further expect that responses for all functional groups will be most pronounced the year after death and then decrease during secondary succession. Finally, we expect that reindeer carcasses will induce a spectral shift in the local vegetation “greenness” that resembles CDIs formation at fresh carcasses (i.e., <1 year old) and succession at older carcasses, i.e., low vegetation greenness at the carcass centre for fresh carcasses and peaking greenness surrounding the centre that steadily fades out with increasing distance (up to a few metres) from the carcass centre for older carcasses.

Materials and methods

Study area

This study was conducted in Adventdalen, including the side valleys Endalen, Todalen, Bolterdalen, and Bjørndalen, in central Spitsbergen ($78^{\circ}13'N$ $15^{\circ}78'E$), Svalbard archipelago (Fig. 1). Only about 15% of the land area is continuously vegetated, 25% consists of barren and sparsely vegetated areas, and about 60% is covered by glaciers (Johansen et al. 2011). The landscape is mountainous with glaciers, and broad glacial valleys with extensive river systems. Local snow conditions combined with hydrological and permafrost-related processes support a variety of habitats with different vegetation compositions (Elvebakk 1994). Four dominant habitat types can be distinguished in the study areas: (1) exposed, well-drained ridges with a sparse vegetation cover dominated by *Dryas octopetala*, (2) heath typically dominated by either *Cassiope tetragona*, *Salix polaris* or *Luzula confusa*, (3) mesic moss tundra dominated by a thick bryophyte layer and high diversity of grass and forb species (such as *Deschampsia alpina*, *Luzula nivalis*, and *Saxifraga* spp.), and (4) wetland dominated

Fig. 2. Conceptual overview of the study designs and data collection methods. Two plots (shown as grids) were overlaid (one over a carcass (right panel), and one at a control location (left panel)). Each grid had 25 subplots, 1 m × 1 m in size. The subplots are categorised into “bands” relating to their position in the grid, i.e., “core” being the centre subplot, “inner” being those directly adjacent to the core subplot (8 subplots), and “edge” being the subplots on the perimeter of the grid (16 subplots). A drone was flown 70 m above the grid pairs, surveying an area of approximately 2 ha.



by most notably moss species such as *Warnstorfia* spp. and *Callicleryon richardsonii* (Elvebakk 1994).

Svalbard has a high-Arctic climate, characterised by low temperatures and precipitation, with average summer and winter temperatures of 4.5 and -13.9°C , respectively (Hanssen-Bauer et al. 2019). Precipitation commonly falls as snow, and the continuous snow cover can persist from October until June (Hanssen-Bauer et al. 2019). Temperature increases in Arctic regions such as Svalbard are amongst the most rapid worldwide and are 3–4 times the global average (Rantanen et al. 2022). Periods of above-zero temperatures in winter with rain have become common (rain-on-snow events) (Peeters et al. 2019), which can result in basal ice covering the vegetation. Such icing events are positively associated with mortality in Svalbard reindeer (Hansen et al. 2011, 2019; Albon et al. 2017).

Study design and data collection

We used two different approaches to assess how Svalbard reindeer carcasses presence affects vegetation cover and plant community composition at 33 sites: (1) vegetation surveys at the carcass site and a nearby control site, and (2) a drone imaging survey over the carcass and its surroundings. Data were collected from 21 July to 3 August 2021. A georeferenced dataset of reindeer carcasses from the Norwegian Polar Institute (Hansen et al. 2019; Å. Pedersen, personal communication, 2021) was used to select carcasses for this study, all of which died from natural causes during late winter/early spring. We chose carcasses that had clear remains of rumen content (i.e., termed CDI) and were reachable on foot or by

boat (i.e., maximum of 8 km from either a road or landing site). The age of the carcasses ranged from approximately half a year to 4 years ($n = 8$ (reindeer dead in 2021) (termed “new”)); and $n = 3$ (2020), $n = 20$ (2019), and $n = 2$ (2017) (termed “old”).

Ground vegetation data

At each of the carcass sites ($N = 33$), we set a 5 m × 5 m grid using a mesh of ropes for the ground vegetation survey. The grid was further subdivided into 1 × 1 m grid cells (subplots) and placed with the central cell covering the carcass centre (i.e., the abdomen or rumen content). The paired control sites ($N = 33$) were placed within 30–50 m from the carcass site in similar vegetation and terrain types (see Fig. 2). For all subplots at the carcass and control sites, we estimated the total cover (to the nearest 5%) of five functional groups, i.e., forbs, graminoids, woody plants, bryophytes, and lichens within each cell. We defined the plant functional groups as following: (1) forbs, including non-graminoid flowering plants without lignin-containing stems; (2) graminoids, including member of Poaceae, Juncaceae, and Cyperaceae; (3) woody plants, including plants with lignin-containing stems (*Betula nana*, *S. polaris*, and *Dryas octopetala*); (4) bryophytes, including mosses, liverworts, and hornworts; and (5) lichens, consisting of all lichenised fungal species. The subplots were categorised into three “bands” relating to their position within the overall grid, i.e., “core” being the centre cell, “inner” being the cells neighbouring the centre cell, and “edge” being the subplots in the outer perimeter (Fig. 2).

Drone imaging data

A DJI Mavic 2 Pro fitted with a Hasselblad L1D-20c RGB camera was flown at approximately 70 m above each carcass and captured some of the surrounding area. The application Pix4D Capture (Pix4D 2022) was used to create a flight route and to collect images for generating orthophotos, with the overlap parameter set to 80% and other settings to default. Agisoft Metashape Professional (software version 1.8.4) was used to generate one orthomosaic for each carcass site, (46 on average per orthomosaic, covering an approximate area of 2 ha and a ground resolution of 1.5 cm/pixel).

Data analysis

Ground vegetation survey

To assess vegetation differences between sites with a carcass and control sites without a carcass, we analysed the vegetation cover data at the subplot (1 m × 1 m) scale. We used generalised linear mixed effects models (glmm) implemented in the R package “glmmTMB” (Magnusson et al. 2021) to assess changes in vegetation cover separately for each functional group between carcass sites and controls. The proportional cover of each functional group within each subplot was the response variable, and two candidate models for each response variable were fitted, i.e., a null model and a model that included an interaction term between type (carcass or control) and band of the grid (core, inner, edge) (eq. 1).

$$(1) \quad \text{Response} \sim \text{Type} * \text{Band} + (1 | \text{Site ID})$$

A single two-way interaction between “type” and “band” was added as we expected there to be a relationship with distance from carcass but not in the case of control sites. Site ID was included as a random effect. The vegetation data were proportional and were fitted with beta regression using the “betareg” R package with a logit link (Cribari-Neto and Zeileis 2010; Magnusson et al. 2021). Model fit was evaluated for the global models by residual diagnostics, including inspection of qq-plots, residuals plotted against predicted values for assessing heteroscedasticity, and test statistics for correct distribution, dispersion, and outliers using the “DHARMA” package in R (Hartig 2022). We chose model simplicity over explanatory power to prevent data overfitting and avoided three-way interactions by principle (Hawkins 2004). The best model was selected using the second-order Akaike’s information criterion corrected for small sample sizes (AICc; Burnham and Anderson 2002) and calculated using the function “aictab” in the AICcmodavg package in R (Mazerolle 2020). Models with $\Delta\text{AICc} < 2$ were regarded to perform equally well (Burnham et al. 2010), and in instances where models performed equally well, the less complex (i.e., the null model) was favoured.

To assess the influence of age, we focused our attention to the “core” subplot (Fig. 2) as we expected very local differences induced by the carcasses ($N = 33$). Bearing in mind our unbalanced age distribution and reduced dataset, the difference between these two age groups was assessed by a Wilcoxon rank-sum test to compare the difference in medians between our two age categories with respect

to the proportional cover of our five vegetation functional groups.

Drone survey

On each orthomosaic, the carcass centre was approximated by selecting the centre of the “core” subplot, as laid by the vegetation surveys. We created distance categories of 0.5 m increment rings from the carcass centre up to 20 m away. Within each distance category, stratified random sampling of pixel values from the orthomosaic was performed (500 points per distance category, 20 000 per site generated). Of these random points, those at distances 15–20 m away from the carcass were considered as control points, i.e., assumed far enough not to be affected by the carcass (5000 control, 15 000 used for modelling).

Deciding which is the best RGB-based vegetation index for assessing tundra (vegetation) greening is not clear, as most of these indices have been developed for agricultural applications (Bendig et al. 2015; Gerardo and de Lima 2023). The Modified Green Red Vegetation Index (MGRVI) and Red Green Blue Vegetation Index (RGBVI) were calculated to assess differences in chlorophyll absorption in relation to carcass proximity (i.e., distance from carcass centre) based on the differences in reflectance in the red, green, and blue wavelengths (Bendig et al. 2015). Plant chlorophyll typically shows high reflectance in the green part of the electromagnetic spectrum, and stronger absorption of red and blue electromagnetic energy (Gao 2006; Bendig et al. 2015). Choosing these indices was intended to function as proxies of chlorophyll quantification in vegetation (Tucker 1979). The Green Leaf Index (GLI) was calculated to assess changes in the vegetation cover in relation to carcass proximity, by showing positive index values for vegetation and negative values for soil and non-vegetated areas (Louhaichi et al. 2001; Eng et al. 2019). Finally, the Excess Red Index (ExR) aims to separate green plants from backgrounds by highlighting redness that can be related to redness in the soil (Meyer and Neto 2008).

The NDVI is a widely used standard for assessing vegetation changes and greening and has formerly been applied in Arctic tundra (Vickers et al. 2016). It involves a simple difference between reflectance in the near-infrared and red wavelengths, which are strongly associated with markers of plant condition such as leaf area, chlorophyll content (Blackburn 2002), and fractional vegetation cover, amongst others (Hansen et al. 2002; Pettorelli et al. 2005). RGB-based spectral vegetation indices have been used for decades, but their application currently increases rapidly due to the uprise of conventional drones (Kazemi and Ghanbari Parmehr 2023). To decide which of the RGB-based indices best reflects tundra productivity and greenness, we calculated each (RGB-based) index (Table 1) on a Sentinel-2 L2A composite (10 × 10 m pixel resolution) over our study area and correlated sample pixel values with a Sentinel-2-derived NDVI on the Google Earth Engine platform. Sentinel 2 would not be able to capture the local carcass effects that we expected and was therefore used instead to inform our choice of RGB-based index. The best-

Table 1. Overview of the four RGB-based vegetation indices tested in this study and their formulas.

Vegetation index	Calculation	References
Modified Green Red Vegetation Index	$MGRVI = \frac{Green^2 - Red^2}{Green^2 + Red^2}$	Bendig et al. (2015)
Red Green Blue Vegetation Index	$RGBVI = \frac{Green^2 - (Red \times Blue)}{Green^2 + (Red \times Blue)}$	Bendig et al. (2015)
Green Leaf Index	$GLI = \frac{(2 \times Green) - Red - Blue}{(2 \times Green) + Red + Blue}$	Louhaichi et al. (2001)
Excess Red Vegetation Index	$ExR = \frac{1.4 \times Red - Green}{Green + Red + Blue}$	Meyer and Neto (2008)

Note: “Green”, “red”, and “blue” refer to the visible light wavelengths and correspond to bands in the DJI Mavic 2 composite.

performing index was selected as the one correlating most strongly with the NDVI. We fitted generalised additive models to assess the relationship between the best-performing vegetation index (response variable) and the distance from the carcass centre in metres (predictor variable), using the R package “mgcv” ([Wood 2011](#)) with the following structure (eq. 2):

$$(2) \quad VI \sim s(\text{distance, by} = \text{age_category}) + s(\text{SiteID, bs} = \text{"re"})$$

We applied a spline smoother on distance to the carcass as categorised by age of carcass (i.e., “old” vs. “new”), and included Site ID as a random effect, with bs = “re” referring to a ridge penalty applied to this random effect. Illumination conditions are challenging to control, particularly in high Arctic regions with low solar angles and frequent cloud cover ([Assmann et al. 2019](#)), and can have significant effects on measured reflectance values ([Ishihara et al. 2015](#)). The random effect was included to account for differences between sites such as habitat type and variations in illumination conditions between drone flights. The models were applied for points up to 15 m distance from the carcass centre. The mean value of the control points (between 15 and 20 m away from the carcass) was plotted as a horizontal asymptote in plots visualising this modelled relationship. Regions where model predictions deviated from this horizontal asymptote were highlighted in the resulting plots (as either as significantly above or below this asymptote) for visualisation.

Results

Carcasses have differential but local impacts on plant functional groups

Graminoids, bryophytes, and lichens responded most strongly to carcasses according to the model selection procedure. For those responses, including the “type” × “band” interaction outperformed null model ([Table 2](#)), and had at least one significant combination of interaction levels (see Appendix A [Table A1](#)). Forb and woody cover did not show a clear response to reindeer carcasses. The null model outperformed the interaction model for forbs, and the interaction model for woody plants was arguably better than the null model ($\Delta AIC = 3.3$, [Table 2](#)). However, given the disparity between this performance and how much better graminoids, bryophytes, and lichens outcompeted their null models (ΔAIC values closer to 100), the evidence for the

woody plants model was considered too weak to show conclusive differences ([Tables 2](#) and [A1](#)).

The regression models showed that for graminoids, lichens, and bryophytes, the induced functional group cover response was local and did not extend more than a few metres from the carcass. Graminoid cover was overall larger at the core of the grid versus its surroundings, whereas the opposite was true for lichens and bryophytes ([Fig. 3](#)). For all responses, the edge band of the carcass grid was not different from control plot values ([Fig. 3](#)). Predicted values from these models fit well in the original data ranges (Appendix A [Fig. A1](#)).

No clear effect of carcass age on proportional cover responses

We anticipated that the differential responses for all functional groups would be more pronounced in older carcasses (i.e., > 1 year old) compared to newer (less than 1 year old); however, we only found that forbs showed a significantly lower median proportion at new sites than at older sites (Appendix A [Fig. A2](#), [Table A2](#)).

Spectral indices can capture secondary succession at CDIs

The best-performing RGB-based vegetation index was the RGBVI (Pearson’s correlation with NDVI of 0.80, $p < 0.001$, see Appendix A [Fig. A3](#)) and was consequently used for assessing vegetation responses at CDIs. The generalised additive modelling of RGBVI against distance, as categorised by age, showed a clear distinction between “old” and “new” carcasses ([Table A3](#), [Fig. 4](#)). Older sites showed an increase in the RGBVI values, albeit very locally (up to 1.3 m), and new sites showed a reduction in greenness up to about 1.8 m.

Discussion

Differential impacts of carcasses on plant functional groups

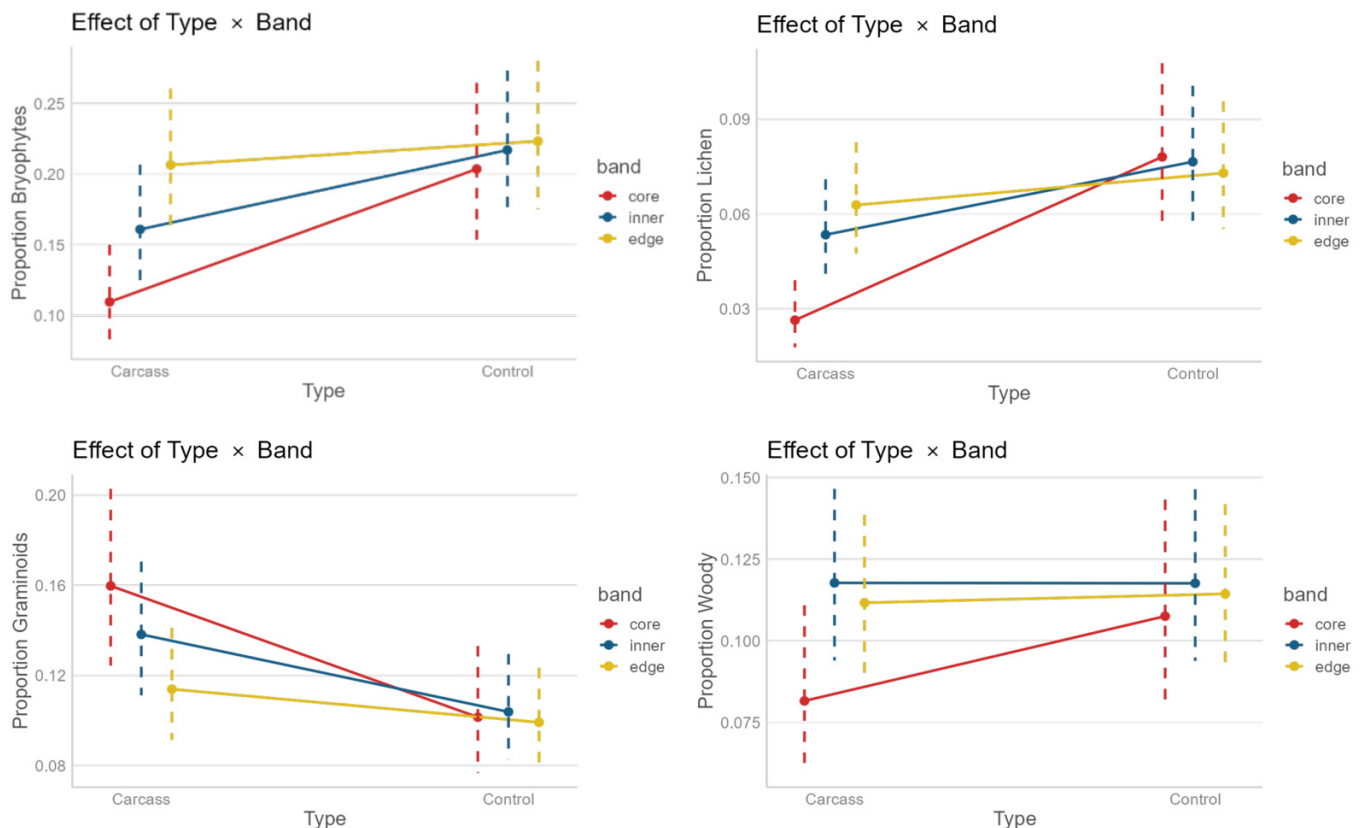
The functional group covers at carcasses versus controls corresponded with our expectations for four out of the five plant functional groups. Bryophytes and lichen showed demonstrable dearth in cover, whereas graminoids thrived with carcass presence—in agreement with previously published work on the responses of these plant functional groups to carcass disturbance, and fertilisation experiments ([Towne](#)

Table 2. Model performance of the assessed models compared to the null model, with each plant functional group as a response.

Functional group	Model	df	AICc	Δ AICc	Weight
Bryophytes	Type \times Band	8	-4031.82	0	1
	Null	3	-3859.89	171.905	0
Graminoids	Type \times Band	8	-5081.16	0	1
	Null	3	-4981.49	99.67	0
Forbs	Null	3	-4500.46	0	0.804
	Type \times Band	8	-4497.63	2.829	0.1956
Lichen	Type \times Band	8	-6686.63	0	1
	Null	3	-6565.87	120.768	0
Woody	Type \times Band	8	-4801.98	0	0.842
	Null	3	-4807.64	3.346	0.158

Note: For each functional group, the test model was a generalised linear mixed effect model, with site as a random effect. The test model had a single two-way interaction between the fixed variables *Type* (carcass vs. control) and *Band* ("core", "inner", or "edge"), i.e., subplot position in the grid. AICc, Akaike information criterion corrected for small sample size; df, degrees of freedom; weight, model weight; Δ AICc, AICc difference values compared to the model with the lowest AICc value.

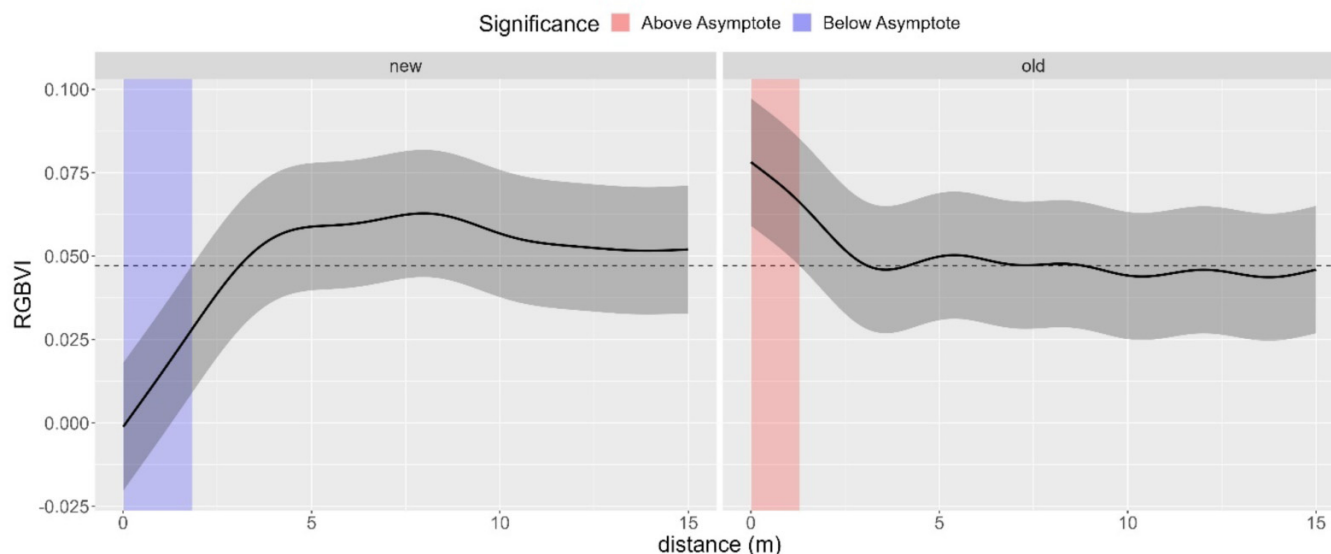
Fig. 3. Predicted effect sizes based on results of the linear mixed effect models for plant functional groups that showed significant responses in proportional cover (0–1), i.e., bryophytes (top left), graminoids (top right), lichen (bottom left), and woody plants (bottom right). The effect of the interaction term *Type* \times *Band* is plotted, with carcass plots compared to control for the three different band categories (i.e., "core", "inner", or "edge"). For carcasses, there was a difference between the core, inner, and edge subplots, whereas for control plots there was no clear distinction. Edge subplots of carcasses approached control values.



2000; Dormann and Woodin 2002; Bump et al. 2009b; Arnberg et al. 2022). Forbs have been shown to have varying responses to carcass presence, depending on biome and carcass age (Towne 2000; Bump et al. 2009b), and generalising forbs as a functional group would perhaps be an oversimplification due

to the variety of life strategies they can present (Jónsdóttir 2011; Bräthen et al. 2021). Among the graminoids, grasses are known to be resilient and ecologically flexible to high degrees of disturbance (Linder et al. 2018), which makes them highly adapted to colonise and persist in carcass-influenced

Fig. 4. Predicted effect sizes based on the generalised additive model of Red Green Blue Vegetation Index (RGBVI) values as a response to distance from carcass centre, with sites categorised by age into “new” (i.e., died that winter, less than 1 year old) and “old” (older than 1 year). The horizontal asymptote marks the mean RGBVI value, based on pixel values at distances of 15–20 m away from the carcasses.



areas. Despite retaining several productive traits (e.g., high species richness, high functional richness, and higher productivity), forbs often have lower abundance compared to grasses a phenomenon, which has been coined the “forb paradox” (Bräthen et al. 2021). Our results show no difference in the cover of forb species with carcass presence, contrary to our expectations of an increase, which may be ascribed to their functional traits, including low cover. Arctic forbs are known to be temperature-dependent during seed production (Arft et al. 1999), and the germination success of viable seeds are dependent on favourable temperature and moisture conditions (Bell and Bliss 1980; Müller et al. 2011). Field germination of Arctic forbs is, thus, reported to be low (Bell and Bliss 1980; Müller et al. 2011), and plant establishment is thought to happen within favourable years (Svoboda and Henry 1987). Our study may have failed to include such years, and this too could contribute to missed potential forb responses. Our results on other functional group responses from High Arctic tundra complemented studies of carcass impacts on these plant functional groups in other biomes.

Response of functional groups to carcass presence is local

We found a local effect of carcass presence on both vegetation composition, i.e., functional group changes in plant cover at core subplots versus edge, and spectral greening, i.e., within the first 2 m. This is in line with other studies documenting local impacts (within 2 m of carcass presence) on chemical concentrations in both soil and plant nitrogen levels (Danell et al. 2002; Wenting et al. 2023). Danell et al. (2002) showed that nitrogen levels in plants (dry matter) was high close to the carcass (<1 m) and decreased with distance, stabil-

ising after 3 m from the carcass. In temperate forest biomes, Melis et al. (2007) also reported a similar local influence induced by carcasses, albeit less dramatic than in tundra and prairie systems, due to high nutrient recycling, higher scavenger densities, and other factors that are likely more limiting in forest biomes, such as light availability. In retrospect, capturing the proportional cover changes in three bands of 1 m × 1 m size may have been too coarse to capture variation smoothly, particularly for the age-related effects (see subsequent paragraph). A band width of 0.5 m as used by Towne (2000) may have better captured variation considering how local these effects are (as they did see a difference between the first 0.5 and 1 m), although 1 m × 1 m has been sufficient for most other studies reviewing carcasses and their local impacts on soil and vegetation nutrients (Danell et al. 2002; Melis et al. 2007). In addition to nutrient deposition, the structure of the carcass itself may contribute to these functional group responses. Fafard et al. (2019) showed that nutrient deposition at Arctic fox dens increased plant biomass, the structures of which in turn promoted snow retention and facilitated species that capitalise on these microhabitats. We might expect a similar influence from carcass structure sheltering certain species from wind in the open tundra and creating microhabitat conditions. How scavengers mitigate this effect in terms of carcass biomass dispersion is unknown, but we would expect great disparity between, for example, Arctic foxes and polar bears in this regard.

No clear effect of carcass age on functional group cover responses

Given our small and unbalanced sample size particularly of the “New” carcass group ($n = 8$), it was difficult to be

conclusive about the change in proportional cover of functional group with carcass age. The Wilcoxon rank-sum test results showed that in our sample, there was a lower median proportional cover of forbs at new carcasses compared to old ($n = 25$, see Appendix AFig. A2, Table A2). As age did appear relevant in our generalised additive model with more fine-scale distance measures than our ground survey, we believe that the sample size and resulting low confidence in our estimates simply missed the effect of age in the functional group proportional cover response rather than it not being present. Other studies demonstrating the influence of carcass age also show how discrete this can be, with Towne (2000) showing clear influence of secondary succession over time. Our selection of 33 carcasses for this study was also restricted to those with a clear “centre”, i.e., rumen remains, which could bias our selection too, particularly for the older carcasses. Given the factors limiting slower microbial and vegetation growth in the Arctic may be time-dependent (Chapin 1983; Propster et al. 2023), our “old” carcasses could still be considered relatively “new”, and perhaps the inclusion of even older carcasses in our sample may have better portrayed the progression of succession, which our relatively “young” carcass sample may have missed.

Spectral indices can capture secondary succession at CDIs

Low and negative RGBVI values seen at the short range for fresh carcasses can be explained by the formation of a CDI, which is locally denuded from vegetation in the short term, and contains higher quantities of bone and fur than at older carcasses (Fig. 4). We expected a dearth of vegetation due to nutrient excess and physical compaction of vegetation (Goyal and Huffaker 1984; Carter et al. 2007), and a green-up with time to show increased productivity compared to their pre-disturbed stage. The model results show that for the first few metres, older carcasses show this “green-up”, with higher RGBVI values than control, very locally to the carcass, which suggests evidence for secondary succession at the CDI over time and age of the carcass (Fig. 4). NDVI has been widely used to monitor “greening” in the Arctic, particularly with respect to climate change-induced warming effects and monitoring of shrub expansion (Jia et al. 2003, 2005; Myers-Smith et al. 2011). Existing research on NDVI and its performance in Arctic domains appears comparable to other more extensively studied biomes. For example, recent ground-truthing efforts in North American tundra systems indicate that NDVI is a good predictor of the biochemical properties of dominant plant functional types, such as the cover and photosynthesis of woody shrubs (Jespersen et al. 2023). On Svalbard too, NDVI has shown a linear relationship with biomass and “greenness” (Johansen and Tømmervik 2014; Vickers et al. 2016). It has also been used as an indicator for vegetation disturbance on tundra from goose herbivory or winter damage, i.e., “rain-on-snow” and thaw-freeze (Eischeid et al. 2021), and detecting disturbances from CDIs are therefore plausible. RGB-based vegetation indices have mostly been assessed in agricultural applications, with RGBVI, in particu-

lar, being strongly correlated with plant height and biomass (Bendig et al. 2015). In our study, this would relate primarily to graminoids, which as the ground survey data confirms, was the functional group with both a large cover composition and an increase at carcass sites compared to controls. Finally, relying on the strong correlation between RGBVI and NDVI in satellite imagery leads us to believe that we could draw similar parallels relating high RGBVI values with high “greenness” and vegetation productivity. Future research efforts could include drone surveys with both RGB and near-infrared sensors to confirm how well the RGBVI functions as a proxy for NDVI here.

Climate change and effects of carrion abundance

Globally, reindeer and caribou have suffered population declines (Vors and Boyce 2009; Uboni et al. 2016). In contrast, the Svalbard reindeer populations have increased over the last century, linked to both Arctic greening and recovery from overharvest (Hansen et al. 2019; Le Moullec et al. 2019). According to climate predictions (Rinke and Dethloff 2008), Svalbard and the Barents Sea are expected to experience some of the highest increases in surface temperatures, particularly in the winter months. Milder temperatures may cause formation of basal ice (when precipitation comes as rain) or deeper snowpacks with implications for reindeer forage access and mortality (Solberg et al. 2001; Putkonen and Roe 2003; Hansen et al. 2011; Albon et al. 2017). Given the high, increasing populations of Svalbard reindeer and the climate predictions, we expect continued elevated reindeer mortality and carcass abundance.

Carrion “pulses”, i.e., spikes of increased abundance, caused by adverse environmental conditions for instance, can encourage consumer dynamic shifts, where populations of scavengers may peak with years of carrion abundance (Ostfeld and Keesing 2000; Moleon et al. 2014). Projected carrion abundance may have cascading effects on scavengers by boosting their populations, which in turn again may affect vegetation dynamics. For example, Arctic foxes engineer hotspots of nutrient concentrations in tundra at their denning sites through excrement and directed distribution of carcass remains for pup rearing (Zhao et al. 2022). Glaucous gulls (*Larus hyperboreus*), another abundant scavenger in this system (Gaden 2023), contribute to “orthogenic drainage”, i.e., the transfer of marine resources to terrestrial areas such as nesting sites (Zmudczyńska-Skarbek et al. 2017; Luoto et al. 2019), and may be important vectors for distributing carrion-derived nutrient across the landscape and diluting “local” CDI effects.

Conclusion

Our results show that reindeer carcasses induce local patches of vegetation change in the Arctic tundra of Svalbard. Carcass distribution is typically not randomly distributed across ecosystems (Bump et al. 2009a; Morant et al. 2022), including in Svalbard, with preliminary results suggesting that reindeer carcasses occur mostly on south-facing slopes of in-

intermediate steepness and with relatively high NDVI values (van den Berg 2022). These patterns may contribute to shaping or maintaining vegetation heterogeneity across the landscape. Our study purely focused on carrion-induced impacts on vegetation. However, carrion typically function as biodiversity hotspots that facilitate ecological interactions between species and organisms of different kingdoms (Barton et al. 2013; Moleon et al. 2014). Very little knowledge currently exists about the ecological role of carrion in the Arctic tundra, and how the environmental context can mediate carcass effects on third parties (Barton et al. 2013). Consequently, estimates of carrion biomass and its spatiotemporal distribution in ecosystems are needed (Barton et al. 2019; Moleon et al. 2020). In the scope of ongoing global change, mass mortality events are on the rise (Barton et al. 2022). Specifically for Svalbard, more unstable winters with increased frequencies of rain on snow events may induce more frequent mass mortality events in Svalbard reindeer (Hansen et al. 2019). Given the forecasted increase in carrion abundance, understanding the ecological dynamics and landscape-level impacts is increasingly relevant in the face of the region's unstable climatic future.

Acknowledgements

No research permits were required to conduct this fieldwork. Any flight within restricted airspace (i.e., >5 km of the airport runway in Longyearbyen) was first cleared with the air traffic control officer present before take-off, and then informed again when the flight was complete. All flights were done by licensed drone pilots only. We thank Stein Tore Pedersen and Jørn Dybdahl for logistic assistance and safety training, and assistants Mie Arnberg, Gunnar Kvifte, Roland Pape, and Andreas Zedrosser for help with field work and safety.

Article information

History dates

Received: 3 April 2024

Accepted: 2 October 2024

Accepted manuscript online: 23 October 2024

Version of record online: 29 January 2025

Notes

This paper is part of a collection entitled Thirty years of Earth System Science in high-Arctic Svalbard: status, trends, and future recommendations.

Copyright

© 2025 The Author(s). This work is licensed under a [Creative Commons Attribution 4.0 International License](#) (CC BY 4.0), which permits unrestricted use, distribution, and reproduction in any medium, provided the original author(s) and source are credited.

Data availability

Data generated and analysed during this study are available in the Dryad repository (doi:10.5061/dryad.1rn8pk142).

Author information

Author ORCIDs

Maya Nisha Situnayake <https://orcid.org/0009-0009-7958-8321>

Marit By <https://orcid.org/0009-0004-8156-8729>

Oddbjørn Larsen <https://orcid.org/0009-0000-1412-1768>

Stijn Sombekke <https://orcid.org/0009-0001-2400-4263>

Lammert Kooistra <https://orcid.org/0000-0001-5549-5993>

Rakel Blaalid <https://orcid.org/0000-0002-3883-8189>

Jan Eivind Østnes <https://orcid.org/0000-0003-0636-6188>

Nuria Selva <https://orcid.org/0000-0003-3389-201X>

Åshild Ønvik Pedersen <https://orcid.org/0000-0001-9388-7402>

Sam M.J.G. Steyaert <https://orcid.org/0000-0001-6564-6361>

Author contributions

Conceptualization: MNS, MB, SS, LK, RB, JEØ, NS, ÅØP, SMJGS

Data curation: MNS, MB, OL, ÅØP

Formal analysis: MNS

Funding acquisition: MB, ÅØP, SMJGS

Investigation: MB, OL, RB, SMJGS

Project administration: MNS, MB, SMJGS

Resources: ÅØP, SMJGS

Software: MNS, MB, OL, SS

Visualization: MNS, SMJGS

Writing – original draft: MNS, NS, ÅØP, SMJGS

Writing – review & editing: MNS, MB, OL, SS, LK, RB, JEØ, NS, ÅØP, SMJGS

Competing interests

The authors declare there are no competing interests.

Funding information

The Norwegian Polar Institute and the Climate Ecological Observatory for Arctic Tundra provided funding for the reindeer abundance surveys and mortality census, and logistics for fieldwork in 2021 (Hansen et al. 2019). Fieldwork expenses for data collection were funded by The Research Council of Norway (Arctic Field Grant 2021) and Nord University (Research Development Grant #300028-111).

References

- Albon, S.D., Irvine, R.J., Halvorsen, O., Langvatn, R., Loe, L.E., Ropstad, E., et al. 2017. Contrasting effects of summer and winter warming on body mass explain population dynamics in a food-limited Arctic herbivore. *Global Change Biology*, 23(4): 1374–1389. doi:10.1111/gcb.13435. PMID: 27426229.
- Arft, A.M., Walker, M.D., Gurevitch, J., Alatalo, J.M., Bret-Harte, M.S., Dale, M., et al. 1999. Responses of tundra plants to experimental warming: meta-analysis of the international tundra experiment. *Ecological Monographs*, 69(4): 491. doi:10.2307/2657227.
- Arnberg, M.P., Eycott, A.E., and Steyaert, S.M.J.G. 2024. From death comes life: large vertebrate carrion enhances seedling establishment in clonal ericaceous shrubs. *Functional Ecology*, 38: 1284–1295. doi:10.1111/1365-2435.14531.
- Arnberg, M.P., Frank, S.C., Blaalid, R., Davey, M.L., Eycott, A.E., and Steyaert, S.M.J.G. 2022. Directed endozoochorous dispersal by scavengers facilitate sexual reproduction in otherwise clonal plants at

- cadaver sites. *Ecology and Evolution*, **12**(1): e8503. doi:[10.1002/ece3.8503](https://doi.org/10.1002/ece3.8503). PMID: [35127028](https://pubmed.ncbi.nlm.nih.gov/35127028/).
- Assmann, J.J., Kerby, J.T., Cunliffe, A.M., and Myers-Smith, I.H. 2019. Vegetation monitoring using multispectral sensors—best practices and lessons learned from high latitudes. *Journal of Unmanned Vehicle Systems*, **7**(1): 54–75. doi:[10.1139/juvs-2018-0018](https://doi.org/10.1139/juvs-2018-0018).
- Barton, P.S., Cunningham, S.A., Lindenmayer, D.B., and Manning, A.D. 2013. The role of carrion in maintaining biodiversity and ecological processes in terrestrial ecosystems. *Oecologia*, **171**(4): 761–772. doi:[10.1007/s00442-012-2460-3](https://doi.org/10.1007/s00442-012-2460-3). PMID: [23007807](https://pubmed.ncbi.nlm.nih.gov/23007807/).
- Barton, P.S., Evans, M.J., Foster, C.N., Pechal, J.L., Bump, J.K., Quagiotto, M.M., and Benbow, M.E. 2019. Towards quantifying carrion biomass in ecosystems. *Trends in Ecology & Evolution*, **34**(10): 950–961. doi:[10.1016/j.tree.2019.06.001](https://doi.org/10.1016/j.tree.2019.06.001).
- Barton, P.S., Rebolini, A., Bonat, S., Mateo-Tomás, P., and Newsome, T.M. 2023. Climate-driven animal mass mortality events: is there a role for scavengers? *Environmental Conservation*, **50**: 1–6. doi:[10.1017/s0376892922000388](https://doi.org/10.1017/s0376892922000388).
- Beasley, J.C., Olson, Z.H., and Devault, T.L. 2012. Carrion cycling in food webs: comparisons among terrestrial and marine ecosystems. *Oikos*, **121**(7): 1021–1026. doi:[10.1111/j.1600-0706.2012.20353.x](https://doi.org/10.1111/j.1600-0706.2012.20353.x).
- Beasley, J.C., Olson, Z.H., and DeVault, T.L. 2015. Ecological role of vertebrate scavengers. In *Carrion ecology, evolution, and their applications*. Edited by E.M. Benbow, J.K. Tomberlin and A.M. Tarone. CRC Press. pp. 107–129.
- Bell, K.L., and Bliss, L.C. 1980. Plant reproduction in a High Arctic environment. *Arctic and Alpine Research*, **12**(1): 1. doi:[10.2307/1550585](https://doi.org/10.2307/1550585).
- Benbow, E.M., Pechal, J.L., and Mohr, R.M. 2015a. Community and landscape ecology of carrion. In *Carrion ecology, evolution, and their applications*. Edited by E.M. Benbow, J.K. Tomberlin and A.M. Tarone. CRC Press. pp. 151–185.
- Benbow, E.M., Tomberlin, J.K., and Tarone, A.M. (Editors). 2015b. *Carrion ecology, evolution, and their applications*. CRC Press.
- Benbow, M.E., Barton, P.S., Ulyshen, M.D., Beasley, J.C., DeVault, T.L., Strickland, M.S., et al. 2019. Necrobiome framework for bridging decomposition ecology of autotrophically and heterotrophically derived organic matter. *Ecological Monographs*, **89**(1): e01331. doi:[10.1002/ecm.1331](https://doi.org/10.1002/ecm.1331).
- Bendig, J., Yu, K., Aasen, H., Bolten, A., Bennertz, S., Broscheit, J., et al. 2015. Combining UAV-based plant height from crop surface models, visible, and near infrared vegetation indices for biomass monitoring in barley. *International Journal of Applied Earth Observation and Geoinformation*, **39**: 79–87. doi:[10.1016/j.jag.2015.02.012](https://doi.org/10.1016/j.jag.2015.02.012).
- Billings, W.D. 1987. Constraints to plant growth, reproduction, and establishment in Arctic environments. *Arctic and Alpine Research*, **19**(4): 357–365. doi:[10.2307/1551400](https://doi.org/10.2307/1551400).
- Blackburn, G.A. 2002. Remote sensing of forest pigments using airborne imaging spectrometer and LIDAR imagery. *Remote Sensing of Environment*, **82**(2–3): 311–321. doi:[10.1016/s0034-4257\(02\)00049-4](https://doi.org/10.1016/s0034-4257(02)00049-4).
- Bräthen, K.A., Pugnaire, F.I., and Bardgett, R.D. 2021. The paradox of forbs in grasslands and the legacy of the mammoth steppe. *Frontiers in Ecology and the Environment*, **19**(10): 584–592. doi:[10.1002/fee.2405](https://doi.org/10.1002/fee.2405).
- Bump, J.K., Barton, P.S., Evans, M.J., Foster, C.N., Pechal, J.L., Quagiotto, M.M., and Benbow, M.E. 2020. Echoing the need to quantify carrion biomass production. *Trends in Ecology & Evolution*, **35**(2): 92–94. doi:[10.1016/j.tree.2019.11.003](https://doi.org/10.1016/j.tree.2019.11.003).
- Bump, J.K., Peterson, R.O., and Vucetich, J.A. 2009a. Wolves modulate soil nutrient heterogeneity and foliar nitrogen by configuring the distribution of ungulate carcasses. *Ecology*, **90**(11): 3159–3167. doi:[10.1890/09-0292.1](https://doi.org/10.1890/09-0292.1).
- Bump, J.K., Webster, C.R., Vucetich, J.A., Peterson, R.O., Shields, J.M., and Powers, M.D. 2009b. Ungulate carcasses perforate ecological filters and create biogeochemical hotspots in forest herbaceous layers allowing trees a competitive advantage. *Ecosystems*, **12**(6): 996–1007. doi:[10.1007/s10021-009-9274-0](https://doi.org/10.1007/s10021-009-9274-0).
- Burnham, K.P., and Anderson, D.R. 2002. *Model selection and multimodel inference: a practical information-theoretic approach*. Springer New York.
- Burnham, K.P., Anderson, D.R., and Huyvaert, K.P. 2010. AIC model selection and multimodel inference in behavioral ecology: some background, observations, and comparisons. *Behavioral Ecology and Sociobiology*, **65**(1): 23–35. doi:[10.1007/s00265-010-1029-6](https://doi.org/10.1007/s00265-010-1029-6).
- Carter, D.O., Yellowlees, D., and Tibbett, M. 2006. Cadaver decomposition in terrestrial ecosystems. *Die Naturwissenschaften*, **94**(1): 12–24. doi:[10.1007/s00114-006-0159-1](https://doi.org/10.1007/s00114-006-0159-1).
- Chapin, F.S. 1983. Direct and indirect effects of temperature on Arctic plants. *Polar Biology*, **2**(1): 47–52. doi:[10.1007/bf00258285](https://doi.org/10.1007/bf00258285).
- Chuvieco, E. 2016. *Fundamentals of satellite remote sensing: an environmental approach*. 2nd ed. CRC Press, Boca Raton.
- Chytrý, M., Schaminée, J.H., and Schwabe, A. 2011. *Vegetation survey: a new focus for Applied Vegetation Science*. Wiley Online Library.
- Cribari-Neto, F., and Zeileis, A. 2010. Beta regression in R. *Journal of Statistical Software*, **34**(2). doi:[10.18637/jss.v034.i02](https://doi.org/10.18637/jss.v034.i02).
- Cruzan, M.B., Weinstein, B.G., Grasty, M.R., Kohn, B.F., Hendrickson, E.C., Arredondo, T.M., and Thompson, P.G. 2016. Small unmanned aerial vehicles (micro-UAVs, drones) in plant ecology. *Applications in Plant Sciences*, **4**(9): 1600041. doi:[10.3732/apps.1600041](https://doi.org/10.3732/apps.1600041).
- Danell, K., Berteaux, D., and Bräthen, K.A. 2002. Effect of muskox carcasses on nitrogen concentration in tundra vegetation. *Arctic*, **55**(4): 389–392. doi:[10.14430/arctic723](https://doi.org/10.14430/arctic723).
- DeVault, T.L., Brisbin, J.I.L., and Rhodes, J.O.E. 2004. Factors influencing the acquisition of rodent carrion by vertebrate scavengers and decomposers. *Canadian Journal of Zoology*, **82**(3): 502–509. doi:[10.1139/z04-022](https://doi.org/10.1139/z04-022).
- Dormann, C.F., and Woodin, S.J. 2002. Climate change in the Arctic: using plant functional types in a meta-analysis of field experiments. *Functional Ecology*, **16**(1): 4–17. doi:[10.1046/j.0269-8463.2001.00596.x](https://doi.org/10.1046/j.0269-8463.2001.00596.x).
- Duffy, J.P., Cunliffe, A.M., DeBell, L., Sandbrook, C., Wich, S.A., Shutler, J.D., et al. 2017. Location, location, location: considerations when using lightweight drones in challenging environments. *Remote Sensing in Ecology and Conservation*, **4**(1): 7–19. doi:[10.1002/rse2.58](https://doi.org/10.1002/rse2.58).
- Eisheid, I., Soininen, E.M., Assmann, J.J., Ims, R.A., Madsen, J., Pedersen, Å.Ø., et al. 2021. Disturbance mapping in Arctic tundra improved by a planning workflow for drone studies: advancing tools for future ecosystem monitoring. *Remote Sensing*, **13**(21): 4466. doi:[10.3390/rs13214466](https://doi.org/10.3390/rs13214466).
- Elveback, A. 1994. A survey of plant associations and alliances from Svalbard. *Journal of Vegetation Science*, **5**(6): 791–802. doi:[10.2307/3236194](https://doi.org/10.2307/3236194).
- Eng, L.S., Ismail, R., Hashim, W., and Baharum, A. 2019. The use of VARI, GLI, and VIgreen formulas in detecting vegetation in aerial images. *International Journal of Technology*, **10**(7): 1385–1394. doi:[10.14716/ijtech.v10i7.3275](https://doi.org/10.14716/ijtech.v10i7.3275).
- Esri. 2024. World Street Map. Version Feb 2, 2024 [online]. Available from <https://www.arcgis.com/home/item.html?id=de26a3cf4cc9451298ea173c4b324736> [accessed 02 February 2024].
- Fafard, P.M., Roth, J.D., Markham, J.H., and Bruun, H.H. 2019. Nutrient deposition on Arctic fox dens creates atypical tundra plant assemblages at the edge of the Arctic. *Journal of Vegetation Science*, **31**(1): 173–179. doi:[10.1111/jvs.12828](https://doi.org/10.1111/jvs.12828).
- Gaden, E.F. 2023. The influence of landscape factors on scavenger community structure and carrion partitioning in the Arctic tundra. M.Sc. Biosciences, Nord University. 64p.
- Gao, J. 2006. Canopy chlorophyll estimation with hyperspectral remote sensing. Ph.D. dissertation, Kansas State University.
- Gerardo, R., and de Lima, I.P. 2023. Applying RGB-based vegetation indices obtained from UAS imagery for monitoring the rice crop at the field scale: a case study in Portugal. *Agriculture*, **13**(10): 1916. doi:[10.3390/agriculture13101916](https://doi.org/10.3390/agriculture13101916).
- Goyal, S.S., and Huffaker, R.C. 1984. Nitrogen toxicity in plants. In *Nitrogen in crop production*. Edited by R.D. Hauck. ASA, CSSA, and SSSA Books. pp. 97–118.
- Hamylton, S.M., Morris, R.H., Carvalho, R.C., Roder, N., Barlow, P., Mills, K., and Wang, L. 2020. Evaluating techniques for mapping island vegetation from unmanned aerial vehicle (UAV) images: pixel classification, visual interpretation and machine learning approaches. *International Journal of Applied Earth Observation and Geoinformation*, **89**: 102085. doi:[10.1016/j.jag.2020.102085](https://doi.org/10.1016/j.jag.2020.102085).
- Hansen, B.B., Aanes, R., Herfindal, I., Kohler, J., and Sæther, B.-E. 2011. Climate, icing, and wild arctic reindeer: past relationships and future prospects. *Ecology*, **92**(10): 1917–1923. doi:[10.1890/11-0095.1](https://doi.org/10.1890/11-0095.1).
- Hansen, B.B., Isaksen, K., Benestad, R.E., Kohler, J., Pedersen, Å.Ø., Loe, L.E., et al. 2014. Warmer and wetter winters: characteristics and implications of an extreme weather event in the High Arctic. *Environ-*

- mental Research Letters, **9**(11): 114021. doi:[10.1088/1748-9326/9/11/114021](https://doi.org/10.1088/1748-9326/9/11/114021).
- Hansen, B.B., Pedersen, Å.Ø., Peeters, B., Le Moullec, M., Albon, S.D., Herfindal, I., et al. 2019. Spatial heterogeneity in climate change effects decouples the long-term dynamics of wild reindeer populations in the high Arctic. *Global Change Biology*, **25**(11): 3656–3668. doi:[10.1111/gcb.14761](https://doi.org/10.1111/gcb.14761).
- Hansen, M.C., DeFries, R.S., Townshend, J.R.G., Sohlberg, R., Dimiceli, C., and Carroll, M. 2002. Towards an operational MODIS continuous field of percent tree cover algorithm: examples using AVHRR and MODIS data. *Remote Sensing of Environment*, **83**(1–2): 303–319. doi:[10.1016/S0034-4257\(02\)00079-2](https://doi.org/10.1016/S0034-4257(02)00079-2).
- Hanssen-Bauer, I., Førland, E.J., Hisdal, H., Mayer, S., Sandø, A.B., and Sorteberg, A. 2019. Climate in Svalbard—a knowledge base for climate adaptation. NCCS report no. 1/2019.
- Hartig, F. 2022. DHARMA: residual diagnostics for hierarchical (multi-level/mixed) regression models.
- Hawkins, D.M. 2004. The problem of overfitting. *Journal of Chemical Information and Computer Sciences*, **44**(1): 1–12. doi:[10.1021/ci0342472](https://doi.org/10.1021/ci0342472).
- Hegland, S.J., and Hamre, L.N. 2018. Scale-dependent effects of landscape composition and configuration on deer-vehicle collisions and their relevance to mitigation and planning options. *Landscape and Urban Planning*, **169**: 178–184. doi:[10.1016/j.landurbplan.2017.09.009](https://doi.org/10.1016/j.landurbplan.2017.09.009).
- Ishihara, M., Inoue, Y., Ono, K., Shimizu, M., and Matsuura, S. 2015. The impact of sunlight conditions on the consistency of vegetation indices in croplands—effective usage of vegetation indices from continuous ground-based spectral measurements. *Remote Sensing*, **7**(10): 14079–14098. doi:[10.3390/rs71014079](https://doi.org/10.3390/rs71014079).
- Janzen, D.H. 1977. Why fruits rot, seeds mold, and meat spoils. *The American Naturalist*, **111**(980): 691–713. doi:[10.1086/283200](https://doi.org/10.1086/283200).
- Jespersen, R.G., Anderson-Smith, M., Sullivan, P.F., Dial, R.J., and Welker, J.M. 2023. NDVI changes in the Arctic: functional significance in the moist acidic tundra of Northern Alaska. *PLoS ONE*, **18**(4): e0285030. doi:[10.1371/journal.pone.0285030](https://doi.org/10.1371/journal.pone.0285030).
- Jia, G.J., Epstein, H.E., and Walker, D.A. 2003. Greening of arctic Alaska, 1981–2001. *Geophysical Research Letters*, **30**(20). doi:[10.1029/2003gl018268](https://doi.org/10.1029/2003gl018268).
- Jia, G.J., Epstein, H.E., and Walker, D.A. 2006. Spatial heterogeneity of tundra vegetation response to recent temperature changes. *Global Change Biology*, **12**(1): 42–55. doi:[10.1111/j.1365-2486.2005.01079.x](https://doi.org/10.1111/j.1365-2486.2005.01079.x).
- Johansen, B., and Tømmervik, H. 2014. The relationship between phytomass, NDVI and vegetation communities on Svalbard. *International Journal of Applied Earth Observation and Geoinformation*, **27**: 20–30. doi:[10.1016/j.jag.2013.07.001](https://doi.org/10.1016/j.jag.2013.07.001).
- Johansen, B.E., Karlsen, S.R., and Tømmervik, H. 2011. Vegetation mapping of Svalbard utilising Landsat TM/ETM+ data. *Polar Record*, **48**(1): 47–63. doi:[10.1017/s0032247411000647](https://doi.org/10.1017/s0032247411000647).
- Jónsdóttir, I.S. 2011. Diversity of plant life histories in the Arctic. *Preslia*, **83**(3): 281–300.
- Kazemi, F., and Ghanbari Parmehr, E. 2023. Evaluation of RGB vegetation indices derived from UAV images for rice crop growth monitoring. *In* ISPRS Annals of the Photogrammetry, Remote Sensing and Spatial Information Sciences X-4/W1-2022. pp. 385–390. doi:[10.5194/isprs-annals-x-4-w1-2022-385-2023](https://doi.org/10.5194/isprs-annals-x-4-w1-2022-385-2023).
- Le Moullec, M., Pedersen, Å.Ø., Stien, A., Rosvold, J., and Hansen, B.B. 2019. A century of conservation: the ongoing recovery of Svalbard reindeer. *The Journal of Wildlife Management*, **83**(8): 1676–1686. doi:[10.1002/jwmg.21761](https://doi.org/10.1002/jwmg.21761).
- Linder, H.P., Lehmann, C.E.R., Archibald, S., Osborne, C.P., and Richardson, D.M. 2018. Global grass (<scp>P</scp>>oaceae) success underpinned by traits facilitating colonization, persistence and habitat transformation. *Biological Reviews*, **93**(2): 1125–1144. doi:[10.1111/brev.12388](https://doi.org/10.1111/brev.12388).
- Louhaichi, M., Borman, M.M., and Johnson, D.E. 2001. Spatially located platform and aerial photography for documentation of grazing impacts on wheat. *Geocarto International*, **16**(1): 65–70. doi:[10.1080/10106040108542184](https://doi.org/10.1080/10106040108542184).
- Luoto, T.P., Rantala, M.V., Kivilä, E.H., Nevalainen, L., and Ojala, A.E.K. 2019. Biogeochemical cycling and ecological thresholds in a High Arctic lake (Svalbard). *Aquatic Sciences*, **81**(2): . doi:[10.1007/s00027-019-0630-7](https://doi.org/10.1007/s00027-019-0630-7).
- Mack, M.C., Schuur, E.A.G., Bret-Harte, M.S., Shaver, G.R., and Chapin, F.S. 2004. Ecosystem carbon storage in arctic tundra reduced by long-term nutrient fertilization. *Nature*, **431**(7007): 440–443. doi:[10.1038/nature02887](https://doi.org/10.1038/nature02887).
- Magnusson, A., Skaug, H., Nielsen, A., Berg, C., Kristensen, K., Maechler, M., et al. 2021. glmmTMB: generalized linear mixed models using template model builder.
- Mazerolle, M.J. 2020. AICcmodavg: Model Selection and Multimodel Inference Based on (Q)AIC(c). Version 2.3-0 [accessed 14 March 2024].
- Mekonnen, Z.A., Riley, W.J., Berner, L.T., Bouskill, N.J., Torn, M.S., Iwahana, G., et al. 2021. Arctic tundra shrubification: a review of mechanisms and impacts on ecosystem carbon balance. *Environmental Research Letters*, **16**(5): 053001. doi:[10.1088/1748-9326/abf28b](https://doi.org/10.1088/1748-9326/abf28b).
- Melis, C., Selva, N., Teurlings, I., Skarpe, C., Linnell, J.D.C., and Andersen, R. 2007. Soil and vegetation nutrient response to bison carcasses in Białowieża Primeval Forest, Poland. *Ecological Research*, **22**(5): 807–813. doi:[10.1007/s11284-006-0321-4](https://doi.org/10.1007/s11284-006-0321-4).
- Meyer, G.E., and Neto, J.C. 2008. Verification of color vegetation indices for automated crop imaging applications. *Computers and Electronics in Agriculture*, **63**(2): 282–293. doi:[10.1016/j.compag.2008.03.009](https://doi.org/10.1016/j.compag.2008.03.009).
- Moleón, M., and Sánchez-Zapata, J.A. 2015. The living dead: time to integrate scavenging into ecological teaching. *Bioscience*, biv101.
- Moleon, M., Sanchez-Zapata, J.A., Selva, N., Donazar, J.A., and Owen-Smith, N. 2014. Inter-specific interactions linking predation and scavenging in terrestrial vertebrate assemblages. *Biological Reviews*, **89**(4): 1042–1054. doi:[10.1111/brev.12097](https://doi.org/10.1111/brev.12097).
- Moleón, M., Selva, N., and Sánchez-Zapata, J.A. 2020. The components and spatiotemporal dimension of carrion biomass quantification. *Trends in Ecology & Evolution*, **35**(2): 91–92. doi:[10.1016/j.tree.2019.10.005](https://doi.org/10.1016/j.tree.2019.10.005).
- Morant, J., Arrondo, E., Cortés-Avizanda, A., Moleón, M., Donazar, J.A., Sánchez-Zapata, J.A., et al. 2023. Large-scale quantification and correlates of ungulate carrion production in the anthropocene. *Ecosystems*, **26**: 383–396. doi:[10.1007/s10021-022-00763-8](https://doi.org/10.1007/s10021-022-00763-8).
- Müller, E., Cooper, E.J., and Alsos, I.G. 2011. Germinability of arctic plants is high in perceived optimal conditions but low in the field. *Botany*, **89**(5): 337–348. doi:[10.1139/b11-022](https://doi.org/10.1139/b11-022).
- Myers-Smith, I.H., Forbes, B.C., Wilmsking, M., Hallinger, M., Lantz, T., Blok, D., et al. 2011. Shrub expansion in tundra ecosystems: dynamics, impacts and research priorities. *Environmental Research Letters*, **6**(4): 045509. doi:[10.1088/1748-9326/6/4/045509](https://doi.org/10.1088/1748-9326/6/4/045509).
- Myneni, R.B., Hall, F.G., Sellers, P.J., and Marshak, A.L. 1995. The interpretation of spectral vegetation indexes. *IEEE Transactions on Geoscience and Remote Sensing*, **33**(2): 481–486. doi:[10.1109/TGRS.1995.8746029](https://doi.org/10.1109/TGRS.1995.8746029).
- Norwegian Polar Institute. n.d. TopoSvalbard [online]. Available from <https://toposvalbard.npolar.no> [accessed 02 February 2024].
- Olea, P.P., Mateo-Tomás, P., and Sánchez-Zapata, J.A. 2019a. Carrion ecology and management. Springer.
- Olea, P.P., Mateo-Tomás, P., and Sánchez-Zapata, J.A. 2019b. Synthesis and future perspectives on carrion ecology and management. *In* Carrion ecology and management. Edited by M.E. Benbow, J.K. Tomberlin and A.M. Tarone. Wildlife Research Monographs. Springer International Publishing, Cham. pp. 275–281.
- Ostfeld, R.S., and Keesing, F. 2000. Pulsed resources and community dynamics of consumers in terrestrial ecosystems. *Trends in Ecology & Evolution*, **15**(6): 232–237. doi:[10.1016/s0169-5347\(00\)01862-0](https://doi.org/10.1016/s0169-5347(00)01862-0).
- Peeters, B., Pedersen, Å.Ø., Loe, L.E., Isaksen, K., Veiberg, V., Stien, A., et al. 2019. Spatiotemporal patterns of rain-on-snow and basal ice in High Arctic Svalbard: detection of a climate–cryosphere regime shift. *Environmental Research Letters*, **14**(1): 015002. doi:[10.1088/1748-9326/aaefb3](https://doi.org/10.1088/1748-9326/aaefb3).
- Peterson, B.G., and Carl, P. 2020. PerformanceAnalytics: econometric tools for performance and risk analysis. Version R package version 2.0.4 [online]. Available from <https://CRAN.R-project.org/package=PerformanceAnalytics> [accessed 14 March 2024].
- Pettorelli, N., Vik, J.O., Mysterud, A., Gaillard, J.-M., Tucker, C.J., and Stenseth, N.C. 2005. Using the satellite-derived NDVI to assess ecological responses to environmental change. *Trends in Ecology & Evolution*, **20**(9): 503–510. doi:[10.1016/j.tree.2005.05.011](https://doi.org/10.1016/j.tree.2005.05.011).
- Pix4D. 2022. Pix4D [online]. Available from <https://www.pix4d.com/> [accessed 14 March 2024].

- Propster, J.R., Schwartz, E., Hayer, M., Miller, S., Monsaint-Queoney, V., Koch, B.J., et al. 2023. Distinct growth responses of tundra soil bacteria to short-term and long-term warming. *Applied and Environmental Microbiology*, **89**(3): e0154322. doi:[10.1128/aem.01543-22](https://doi.org/10.1128/aem.01543-22).
- Putkonen, J., and Roe, G. 2003. Rain-on-snow events impact soil temperatures and affect ungulate survival. *Geophysical Research Letters*, **30**(4): 1188. doi:[10.1029/2002gl016326](https://doi.org/10.1029/2002gl016326).
- Rantanen, M., Karpechko, A.Y., Lipponen, A., Nordling, K., Hyvärinen, O., Ruosteenoja, K., et al. 2022. The Arctic has warmed nearly four times faster than the globe since 1979. *Communications Earth & Environment*, **3**(1). doi:[10.1038/s43247-022-00498-3](https://doi.org/10.1038/s43247-022-00498-3).
- Reimers, E. 1983. Mortality in Svalbard reindeer. *Holarctic Ecology*, **6**(2): 141–149.
- Rinke, A., and Dethloff, K. 2008. Simulated circum-arctic climate changes by the end of the 21st century. *Global and Planetary Change*, **62**(1–2): 173–186. doi:[10.1016/j.gloplacha.2008.01.004](https://doi.org/10.1016/j.gloplacha.2008.01.004).
- Selva, N., Jedrzejewska, B., Jedrzejewski, W., and Wajrak, A. 2005. Factors affecting carcass use by a guild of scavengers in European temperate woodland. *Canadian Journal of Zoology*, **83**(12): 1590–1601. doi:[10.1139/z05-158](https://doi.org/10.1139/z05-158).
- Solberg, E.J., Jordhøy, P., Strand, O., Aanes, R., Loison, A., Sæther, B.E., and Linnell, J.D.C. 2001. Effects of density-dependence and climate on the dynamics of a Svalbard reindeer population. *Ecography*, **24**(4): 441–451. doi:[10.1111/j.1600-0587.2001.tb00479.x](https://doi.org/10.1111/j.1600-0587.2001.tb00479.x).
- Steyaert, S.M.J.G., Frank, S.C., Puliti, S., Badia, R., Arnberg, M.P., Beard-sley, J., et al. 2018. Special delivery: scavengers direct seed dispersal towards ungulate carcasses. *Biology Letters*, **14**(8): 20180388. doi:[10.1098/rsbl.2018.0388](https://doi.org/10.1098/rsbl.2018.0388).
- Steyaert, S.M.J.G., Zedrosser, A., Elfström, M., Ordiz, A., Leclerc, M., Frank, S.C., et al. 2016. Ecological implications from spatial patterns in human-caused brown bear mortality. *Wildlife Biology*, **22**(4): 144–152. doi:[10.2981/wlb.00165](https://doi.org/10.2981/wlb.00165).
- Svoboda, J., and Henry, G.H.R. 1987. Succession in marginal arctic environments. *Arctic and Alpine Research*, **19**(4): 373. doi:[10.2307/1551402](https://doi.org/10.2307/1551402).
- Towne, E.G. 2000. Prairie vegetation and soil nutrient responses to ungulate carcasses. *Oecologia*, **122**(2): 232–239. doi:[10.1007/PL00008851](https://doi.org/10.1007/PL00008851).
- Tucker, C.J. 1979. Red and photographic infrared linear combinations for monitoring vegetation. *Remote Sensing of Environment*, **8**(2): 127–150. doi:[10.1016/0034-4257\(79\)90013-0](https://doi.org/10.1016/0034-4257(79)90013-0).
- Ubani, A., Horstkotte, T., Kaarlejärvi, E., Sévêque, A., Stammer, F., Olofsson, J., et al. 2016. Long-term trends and role of climate in the population dynamics of eurasian reindeer. *PLoS ONE*, **11**(6): e0158359. doi:[10.1371/journal.pone.0158359](https://doi.org/10.1371/journal.pone.0158359).
- van den Berg, J. 2022. Modelling the spatial distribution of reindeer cadavers in the Arctic tundra. 3337. Arctic Field Grant Report. REINCAR—carcass ecology in nordic ecosystems (REINCAR).
- van Klink, R., van Laar-Wiersma, J., Vorst, O., and Smit, C. 2020. Rewilding with large herbivores: positive direct and delayed effects of carrion on plant and arthropod communities. *PLoS ONE*, **15**(1): e0226946. doi:[10.1371/journal.pone.0226946](https://doi.org/10.1371/journal.pone.0226946).
- Vickers, H., Høgda, K.A., Solbø, S., Karlsen, S.R., Tømmervik, H., Aanes, R., and Hansen, B.B. 2016. Changes in greening in the high Arctic: insights from a 30 year AVHRR max NDVI dataset for Svalbard. *Environmental Research Letters*, **11**(10): 105004. doi:[10.1088/1748-9326/11/10/105004](https://doi.org/10.1088/1748-9326/11/10/105004).
- Vors, L.S., and Boyce, M.S. 2009. Global declines of caribou and reindeer. *Global Change Biology*, **15**(11): 2626–2633. doi:[10.1111/j.1365-2486.2009.01974.x](https://doi.org/10.1111/j.1365-2486.2009.01974.x).
- Wenting, E., Jansen, P.A., Laugeman, M.J.B., and van Langevelde, F. 2023. Leakage of nutrients into the soil due to carrion decomposition can enhance plant growth. *Journal of Soil Science and Plant Nutrition*, **23**(4): 6874–6879. doi:[10.1007/s42729-023-01430-0](https://doi.org/10.1007/s42729-023-01430-0).
- Wilson, E.E., and Wolkovich, E.M. 2011. Scavenging: how carnivores and carrion structure communities. *Trends in Ecology & Evolution*, **26**(3): 129–135. doi:[10.1016/j.tree.2010.12.011](https://doi.org/10.1016/j.tree.2010.12.011).
- Wood, S.N. 2011. Fast stable restricted maximum likelihood and marginal likelihood estimation of semiparametric generalized linear models. *Journal of the Royal Statistical Society Series B: Statistical Methodology*, **73**(1): 3–36. doi:[10.1111/j.1467-9868.2010.00749.x](https://doi.org/10.1111/j.1467-9868.2010.00749.x).
- Xia, J., Wang, Y., Dong, P., He, S., Zhao, F., and Luan, G. 2022. Object-oriented canopy gap extraction from UAV images based on edge enhancement. *Remote Sensing*, **14**(19): 4762. doi:[10.3390/rs14194762](https://doi.org/10.3390/rs14194762).
- Zhang, X., Zhang, F., Qi, Y., Deng, L., Wang, X., and Yang, S. 2019. New research methods for vegetation information extraction based on visible light remote sensing images from an unmanned aerial vehicle (UAV). *International Journal of Applied Earth Observation and Geoinformation*, **78**: 215–226. doi:[10.1016/j.jag.2019.01.001](https://doi.org/10.1016/j.jag.2019.01.001).
- Zhao, S.-T., Johnson-Bice, S.M., and Roth, J.D. 2022. Foxes engineer hotspots of wildlife activity on the nutrient-limited Arctic tundra. *Global Ecology and Conservation*, **40**: e02310. doi:[10.1016/j.gecco.2022.e02310](https://doi.org/10.1016/j.gecco.2022.e02310).
- Zmudczyńska-Skarbek, K., Barcikowski, M., Drobniak, S.M., Gwiazdowicz, D.J., Richard, P., Skubała, P., and Stempniewicz, L. 2017. Transfer of ornithogenic influence through different trophic levels of the Arctic terrestrial ecosystem of Bjørnøya (Bear Island), Svalbard. *Soil Biology and Biochemistry*, **115**: 475–489. doi:[10.1016/j.soilbio.2017.09.008](https://doi.org/10.1016/j.soilbio.2017.09.008).

Appendix A

Table A1. Parameter estimates and the standard error for the best-performing mixed effect models (GLMMs) per functional group (i.e., proportional cover as a response).

Predictors	Bryophytes				Graminoids				Lichen				Woody			
	Est	SE	<i>p</i>		Est	SE	<i>p</i>		Est	SE	<i>p</i>		Est	SE	<i>p</i>	
(Intercept)	−2.09	0.18	<0.001	***	−1.66	0.15	<0.001	***	−3.61	0.21	<0.001	***	−2.42	0.17	<0.001	***
Type (carcass), Band (core)	Reference				Reference				Reference				Reference			
Band (inner)	0.44	0.11	<0.001	***	−0.17	0.09	0.057	.	0.73	0.15	<0.001	***	0.41	0.13	0.001	**
Band (edge)	0.75	0.10	<0.001	***	−0.39	0.09	<0.001	***	0.91	0.15	<0.001	***	0.35	0.13	0.006	**
Type (control)	0.73	0.13	<0.001	***	−0.52	0.13	<0.001	***	1.14	0.18	<0.001	***	0.30	0.17	0.068	.
Type (control) × Band (inner)	−0.36	0.14	0.009	**	0.20	0.14	0.150		−0.75	0.18	<0.001	***	−0.31	0.18	0.081	.
Type (control) × Band (edge)	−0.63	0.13	<0.001	***	0.37	0.13	0.006	**	−0.98	0.18	<0.001	***	−0.28	0.17	0.106	
Random Effects																
τ_{00}	0.88 _{Site ID}				0.70 _{Site ID}				0.85 _{Site ID}				0.70 _{Site ID}			
<i>N</i>	33 _{Site ID}				33 _{Site ID}				33 _{Site ID}				33 _{Site ID}			

Note: Predictors included in the analysis were the interaction between the fixed, categorical variables, *Type* (i.e., carcass or control) and *Band* (i.e., “core,” “inner” or “edge,” referring to the position of the subplot cell in the 5 × 5 m grid), and the fixed effect *Age* (i.e., “old” or “new” carcasses). The model for forb proportional cover is excluded as the null model outperformed the proposed model. The model reference level was set to new carcass core subplot.

Est, estimates (for fixed effects); *SE*, standard error of estimates; *p*, *p* value indicating significance around the fixed effect.

τ_{00} , variance of the random effect; *N*, number of categories included in the random effect.

Significance codes: 0 “***” 0.001 “**” 0.01 “*” 0.05 “.” 0.1 “.” 1.

Table A2. Wilcoxon rank-sum test results comparing the core plots of old and new carcasses, for the different functional groups.

Wilcoxon rank sum test	Median		Effect size	Z	p value	Magnitude
	New	Old				
Bryophytes	0.125	0.100	0.14	0.80	0.42	Small
Graminoids	0.125	0.200	0.32	-1.86	0.06	Moderate
Forbs	0.100	0.150	0.45	-2.58	0.01	Moderate
Lichen	0.030	0.050	0.09	0.49	0.62	Small
Woody	0.150	0.100	0.16	0.90	0.37	Small

Note: Only forbs showed a significant result ($p < 0.05$), although graminoids also showed a moderate difference with higher median proportions at old carcasses compared to new. Z: Z-statistic; *Effect size*: Z/\sqrt{N} . Varies from 0 to close to 1; *Magnitude*: effect size ranges categorized, i.e., 0.10–<0.3 (small magnitude), 0.30–<0.5 (moderate magnitude), and ≥ 0.5 (large magnitude); p value: test significance value.

Table A3. Parameter estimates of the generalised additive model of RGBVI as a response variable, and distance from carcass centre as the fixed effect.

	Estimate	SE	p value
(Intercept)	0.05	0.01	<0.0001
	Eff. dF	F	p value
s(Distance) (new)	8.2	662.1	<0.0001
s(Distance) (old)	8.9	568.6	<0.0001
s(Site ID)	31.9	3408.4	<0.0001
Adjusted $R^2 = 0.195$, deviance explained = 19.5%			

Note: Sites were categorised by Age, i.e., “new” and “old” carcasses. A spline smoother was applied, and Site ID was included as a random effect. *Est.*, estimates for fixed effects; *SE*, standard error around the estimates; *Eff DF*, effective degrees of freedom for the model terms—if higher than one, this suggests that the relationship is non-linear; *F*, F-statistic value testing the significance of the smoothed term; *p* value, p value indicating significance around the fixed/smoothed terms.

Fig. A1. Fitted model results (grey error bars) versus the raw data (boxplots, grouped by Type and Band), for each of the four functional group's proportional data. The width of the boxplots reflects the data size, with 1 “core”, 8 “inner”, and 16 “edge” observations per site (2×33). Forbs are excluded as the null model was the best performer.

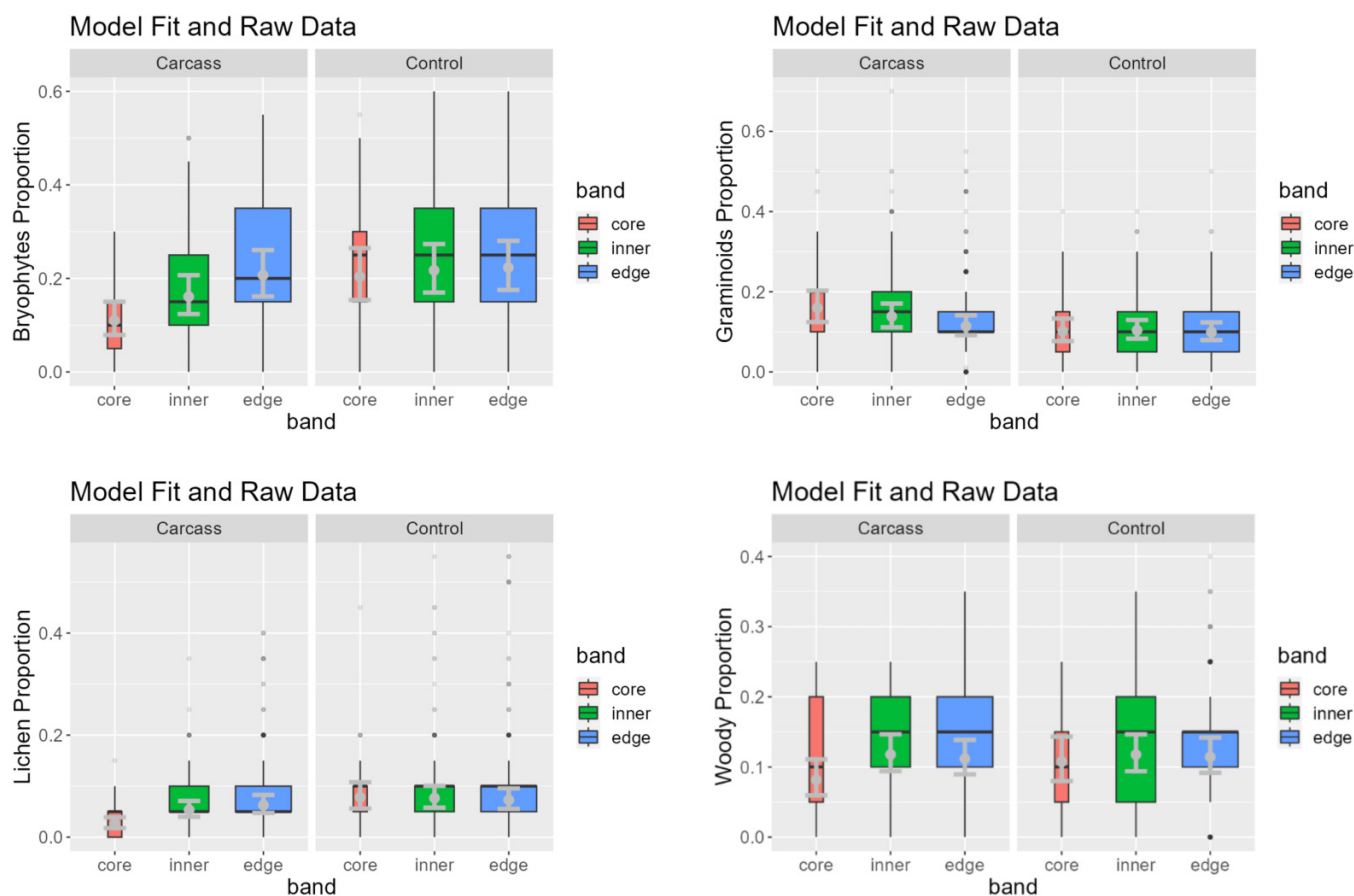


Fig. A2. The proportional cover (0–1) of the vegetation functional groups, as categorized by age. There was no statistically significant difference in median proportional cover between old and new carcasses for any of the functional groups, except for forbs, which had lower cover at new carcasses compared to old sites.

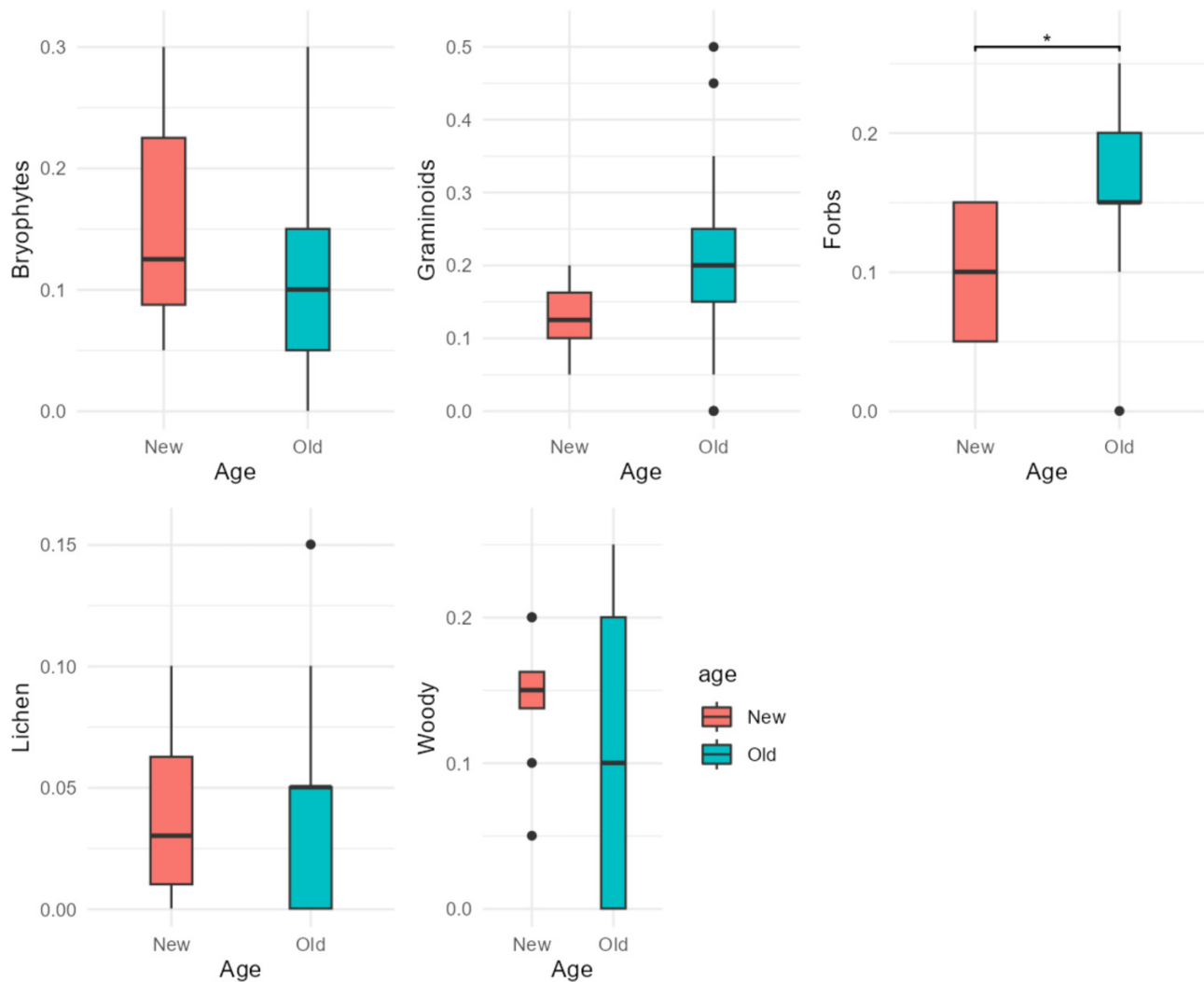


Fig. A3. Correlation matrix visualized for the spectral indices calculated from a Sentinel-2 L2A scene over the study area. Normalised Difference Vegetation Index (NDVI), as widely used vegetation index for vegetation health and productivity, is our baseline here. 3 RGB-computed vegetation indices are compared with NDVI. Here, Red Green Blue Vegetation Index (RGBVI) is the most strongly positively correlated index (Pearson's correlation $r = 0.80$, $p < 0.001$). The extreme negative NDVI values are caused by small snow patches in the satellite image at higher elevations and are not in our study. The pairs to the lower left show bivariate scatterplots with a fitted line, and the top right show the Pearson's correlation values and their significance (where *** denotes a p value significance < 0.001). This plot was created using the R-package "PerformanceAnalytics" (Peterson and Carl 2020).

